Organic & Biomolecular Chemistry

Cite this: *Org. Biomol. Chem.*, 2011, **9**, 4085

www.rsc.org/obc

PAPER

One-electron oxidation of ferrocenes by short-lived *N*-oxyl radicals. The role of structural effects on the intrinsic electron transfer reactivities†‡

Enrico Baciocchi,[a] Massimo Bietti,[b] Claudio D'Alfonso,[a] Osvaldo Lanzalunga,*[a] Andrea Lapi[a] and Michela Salamone[b]

Received 27th December 2010, Accepted 6th April 2011
DOI: 10.1039/c0ob01257b

A kinetic study of the one electron oxidation of substituted ferrocenes (FcX: X = H, COPh, COMe, CO_2Et, $CONH_2$, CH_2OH, Et, and Me_2) by a series of *N*-oxyl radicals (succinimide-*N*-oxyl radical (SINO), maleimide-*N*-oxyl radical (MINO), 3-quinazolin-4-one-*N*-oxyl radical (QONO) and 3-benzotriazin-4-one-*N*-oxyl radical (BONO)), has been carried out in CH_3CN. *N*-oxyl radicals were produced by hydrogen abstraction from the corresponding *N*-hydroxy derivatives by the cumyloxyl radical. With all systems, the rate constants exhibited a satisfactory fit to the Marcus equation allowing us to determine self-exchange reorganization energy values ($\lambda_{NO^{\bullet}/NO^{-}}$) which have been compared with those previously determined for the PINO/$PINO^-$ and BTNO/$BTNO^-$ couples. Even small modification of the structure of the *N*-oxyl radicals lead to significant variation of the $\lambda_{NO^{\bullet}/NO^{-}}$ values. The $\lambda_{NO^{\bullet}/NO^{-}}$ values increase in the order BONO < BTNO < QONO < PINO < SINO < MINO which do not parallel the order of the oxidation potentials. The higher $\lambda_{NO^{\bullet}/NO^{-}}$ values found for the MINO and SINO radicals might be in accordance with a lower degree of spin delocalization in the radicals MINO and SINO and charge delocalization in the anions $MINO^-$ and $SINO^-$ due to the absence of an aromatic ring in their structure.

Introduction

Hydrogen atom transfer (HAT) processes promoted by short-lived *N*-oxyl radicals have received a great attention in recent years. In particular they represent the key step in the synthetically useful metal catalyzed aerobic oxidation of a wide variety of organic substrates promoted by the phthalimide-*N*-oxyl radical (PINO).[1] HAT reactions by *N*-oxyl radicals are also relevant in the oxidative degradation of lignin promoted by the laccase/O_2 system mediated by *N*-hydroxy derivatives, a process which has a potential application in the pulp and paper industry.[2] In this context it has to be noted that several laccase/*N*-hydroxy mediator systems have been investigated and found valuable in the aerobic oxidation of non-phenolic lignin models and of lignin itself from industrial wood pulp.[3] The laccase/*N*-hydroxy mediator systems have also been applied in organic synthesis,[4] and in the degradation of organic pollutants.[5]

The reactivity of a wide variety of *N*-oxyl radicals in HAT processes from both C–H[6] and phenolic O–H bonds[7,8] has been the subject of several studies and much information is now available in this respect.

We have recently shown that with easily oxidizable substrates short-lived aminoxyl radicals like PINO and benzotriazole-*N*-oxyl radical (BTNO) can also operate by an electron transfer (ET) mechanism as found in the *N*-demethylation of *N*,*N*-dimethylanilines.[9,10] This observation led us to investigate the intrinsic ET properties of PINO and BTNO through a careful study of the oxidation of a series of ferrocenes to the corresponding ferrocenium cations, a *bona fide* electron transfer reaction.[11,12] A remarkable result was that the intrinsic ET reactivity of BTNO was significantly higher than that of PINO in spite of the fact that the latter is a slightly better oxidant than the former.

In an attempt to gain more information on how the structure of short-lived *N*-oxyl radicals may influence the ET properties of these reactive species we have considered worthwhile to extend the previous studies to a larger series of *N*-oxyl radicals, namely to the succinimide-*N*-oxyl (SINO, **1**), maleimide-*N*-oxyl (MINO, **2**), 3-quinazolin-4-one-*N*-oxyl (QONO, **3**) and 3-benzotriazin-4-one-*N*-oxyl (BONO, **4**) radicals whose structures are shown in Chart 1 together with those of PINO (**5**) and BTNO (**6**).

The same approach previously used for the ET reactions promoted by PINO and BTNO has been used to acquire information on the self-exchange intrinsic barrier for the extended series of $R_2NO^{\bullet}/R_2NO^-$ couples, thus, in this paper we now report on a

[a]*Dipartimento di Chimica, Sapienza Università di Roma and Istituto CNR di Metodologie Chimiche (IMC-CNR), Sezione Meccanismi di Reazione, c/o Dipartimento di Chimica, Sapienza Università di Roma, piazzale A. Moro, 5 I-00185, Rome, Italy. E-mail: osvaldo.lanzalunga@uniroma1.it*

[b]*Dipartimento di Scienze e Tecnologie Chimiche, Università "Tor Vergata", Via della Ricerca Scientifica, I-00133, Rome, Italy*

† This paper is dedicated to the memory of Professor Athel Beckwith, who contributed much to the knowledge of the structural effects on the free radical reactivity.

‡ Electronic supplementary information (ESI) available. See DOI: 10.1039/c0ob01257b

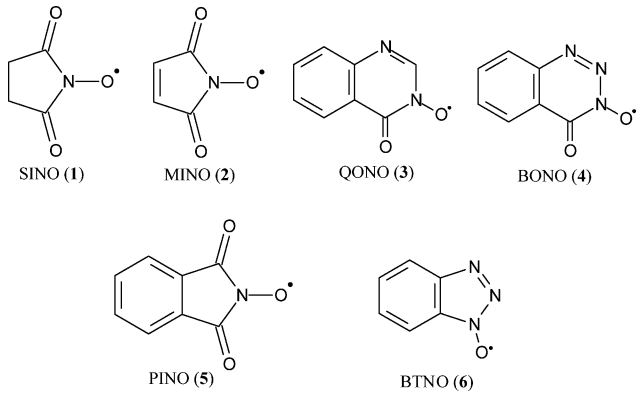

Chart 1

laser flash photolysis (LFP) study of the one electron oxidation of a series of substituted ferrocenes (FcX: X = H, COPh, COMe, CO_2Et, $CONH_2$, CH_2OH, Et, and Me_2) by the *N*-oxyl radicals **1–4** in MeCN (eqn (1)).

Results

The analysis of the ET properties of the *N*-oxyl radicals **1–4** has required the determination of the redox potentials of these species by cyclic voltammetry (CV) under the same experimental conditions used for the analysis of the redox potential of the PINO/$PINO^-$ and BTNO/$BTNO^-$ couples.[11,12] Thus, the measurements were carried out with a solution of the *N*-hydroxy derivatives (2.0 mM) and Bu_4NBF_4 (0.1 M) as the supporting electrolyte in MeCN in the presence of collidine (4 mM) that serves to deprotonate the hydroxylamine moiety giving the corresponding NO^- anion. An Ag/AgCl (KCl 3 M) electrode was used as reference and the scan rate was 500 mV s^{-1}. Reversibility was observed in all cases and the pertinent CVs are reported in the ESI (Figure S1‡). The E° values referred to SCE are reported in Table 1.

As in the one-electron oxidation of ferrocenes promoted by PINO and BTNO, the reactions were too fast to be followed spectrophotometrically and the kinetic studies were therefore carried out by laser flash photolysis (LFP), with the *N*-oxyl radicals **1–4** being produced by hydrogen atom abstraction from the corresponding *N*-hydroxy derivatives **1H–4H**: *N*-hydroxysuccinimide (NHSI), *N*-hydroxymaleimide (NHMI), 3-hydroxyquinazolin-4-one (NHQO) and 3-hydroxybenzotriazin-4-one (NHBO), to the cumyloxyl radical generated by 355 nm LFP of dicumyl peroxide (eqs 2–3 in Scheme 1). Hydrogen atom transfer from the *N*-hydroxy derivatives to the cumyloxyl radical occurs in competition with β-scission of the latter leading to the formation of acetophenone and a methyl radical (eq 4, $k_\beta \sim 6.5 \times 10^5$ s^{-1} in CH_3CN[13]).

Table 1 Reduction potentials for *N*-oxyl radicals **1–6**

N-Oxyl radical	E° (V *vs.* SCE)[a]
SINO (**1**)	0.92
MINO (**2**)	0.77
QONO (**3**)	0.84
BONO (**4**)	0.77
PINO (**5**)	0.69[b]
BTNO (**6**)	0.63[c]

[a] Determined in CH_3CN at 25 °C. R_2N-OH (2.0 mM) and Bu_4NBF_4 (0.1 M) as supporting electrolyte in the presence of collidine (4 mM). Scan rate 500 mV s^{-1}. Error ±0.01 V. [b] Ref. 11 [c] Ref. 12.

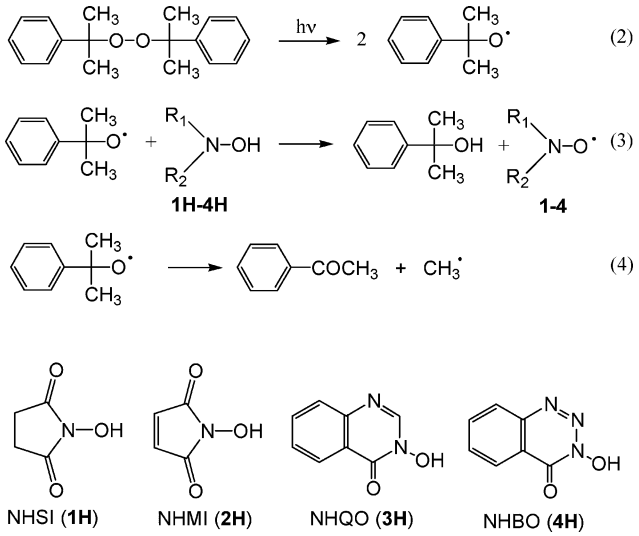

Scheme 1

The time-resolved spectra obtained in a LFP experiment carried out with a solution of dicumyl peroxide (0.9 M) and NHBO (2.5 mM) are reported in Fig. 1, where it can be observed that the cumyloxyl radical, characterized by an absorption maximum at 490 nm (empty circles),[14] undergoes a first-order decay accompanied by a corresponding buildup of optical density at λ = 380 nm due the the absorption of the BONO radical (filled circles). An isosbestic point can be identified at λ = 405 nm. A similar situation (Figure S2 in the ESI‡) was found for the reaction of NHQO with

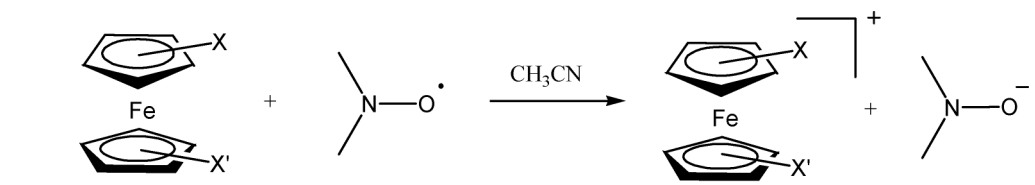

X=X'=H X=CONH2 X'=H
X=X'=Me X=CO2Et X'=H
X=Et X'=H X=COMe X'=H
X=CH2OH X'=H X=COPh X'=H

(1)

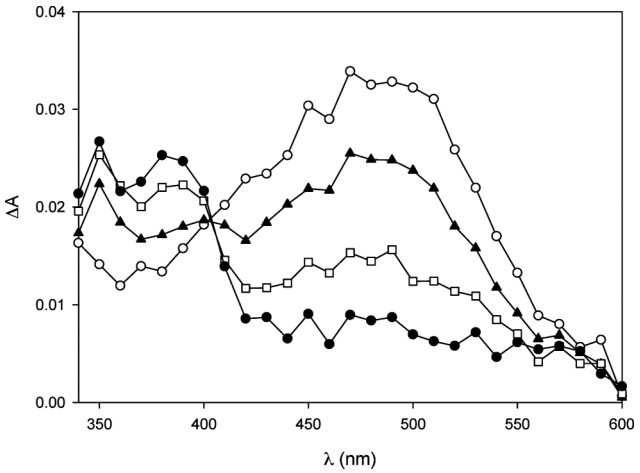

Fig. 1 Transient absorption spectra measured 128 ns (empty circles), 608 ns (filled triangles), 1.8 μs (empty squares) and 8.0 μs (filled circles) after 355 nm laser excitation of a solution of dicumyl peroxide (0.9 M) and NHBO (2.5 mM) in CH_3CN at 25 °C under N_2.

the cumyloxyl radical which forms QONO absorbing at 480 nm. With NHSI and NHMI it was only possible to observe the decay of the cumyloxyl radical due to the weak absorption of the SINO and MINO radicals.

The observed rate constants (k_{obs}) were measured by following the decrease of the optical density at 490 nm, as a function of the concentration of **1H–4H** in the range 0.5–7 mM. Clean first-order decays were observed, and a linear dependency of k_{obs} on the concentration of **1H–4H** was obtained (see figures S3–S6 in the ESI‡). From the slope of these plots the second order rate constants for the HAT process (k_H) were determined. These values are reported in Table 2 together with those previously determined for the HAT process from *N*-hydroxyphthalimide[11] and 6-CF_3-1-hydroxybenzotriazole.[12]

It can be observed that all the rate constants are similar, the difference between the more reactive 6-CF_3-HBT and the less reactive NHQO and NHBO being less than one order of magnitude. On the basis of these values it is possible to suggest that NHMI, NHQO and NHBO are characterized by an O–H BDE comparable with that of NHPI.[15] Accordingly, almost identical liquid phase O–H BDE values for NHPI (83.3 kcal mol^{-1}) and NHMI (83.5 kcal mol^{-1}) were obtained from G3B3 calculations.[16] Interestingly the rate constant for HAT from NHSI to the cumyloxyl radical is higher than that observed for HAT from NHPI and NHMI even though the calculated O–H BDE for NHSI is ca 5 kcal mol^{-1} higher than the O–H BDEs of NHPI and NHMI.[17,18] Additional experimental and computational studies are required in order to explain this discrepancy.

Table 2 Second order rate constants for hydrogen atom transfer from *N*-hydroxy derivatives to the cumyloxyl radical in CH_3CN at 25 °C

R_2N–OH	k_H ($M^{-1}s^{-1}$)[a]
NHSI	$1.6 \pm 0.3 \times 10^8$
NHMI	$4.3 \pm 0.7 \times 10^7$
NHQO	$3.6 \pm 0.3 \times 10^7$
NHBO	$3.6 \pm 0.5 \times 10^7$
NHPI	5.1×10^{7a}
6-CF_3-HBT	2.2×10^{8b}

[a] Errors are reported as twice the standard deviation. [b] Ref. 11 [c] Ref. 12.

The reactions of the *N*-oxyl radicals with the ferrocene donors were studied in MeCN by LFP. The $R_2NO^{\bullet}$ absorptions are stable on the millisecond timescale. After addition of the ferrocene donor FcX, the time-resolved spectra showed a well-defined buildup of the absorption at λ = 320–350 nm and 600–700 nm due to the formation of the ferrocenium ions[20] which is indicative of the occurrence of the ET reaction (eqn (1)), as described previously for the reactions of PINO and BTNO.

In Fig. 2 the time-resolved absorption spectra observed after 355 nm LFP of dicumyl peroxide (1 M), NHQO (3 mM) and ferrocene (0.1 mM) are reported. The absorption spectrum of the QONO radical, recorded 1.6 μs after the laser pulse (empty circles), undergoes a pseudo first-order decay (inset b) accompanied by the formation of the ferrocenium ion (inset a) which displays a strong absorption at λ < 350 nm and the characteristic less intense visible absorption band at λ_{max} = 620 nm.[21]

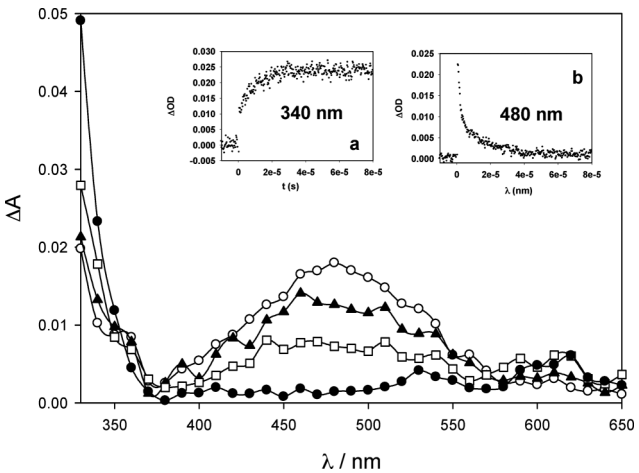

Fig. 2 Time-resolved absorption spectra observed after 355 nm LFP of an N_2-saturated CH_3CN solution (T = 25 °C) containing dicumyl peroxide (1 M), NHQO (3 mM) and ferrocene (0.1 mM), at 1.6 μs (empty circles), 2.3 μs (filled triangles), 5.7 μs (empty squares) and 43 μs (filled circles) after the 8 ns, 20 mJ laser flash. Inset **a**: buildup of the absorption of the ferrocenium ion at 340 nm. Inset **b**: decay of the absorption of QONO at 480 nm.

Two isosbestic points can be identified at λ = 370 and 570 nm. Time-resolved absorption spectra observed after 355 nm LFP of dicumyl peroxide (1 M), NHBO (5 mM) and ethylferrocene carboxylate (0.1 mM) are reported in Figure S7 in the ESI.‡

Kinetic studies were carried out by following the buildup of the ferrocenium ions between 330 and 350 nm and, with the BONO radical by following the decay of the *N*-oxyl radical visible absorption band. With BONO the kinetic study was limited to ferrocenes substituted with electron withdrawing substituent because FcH was too reactive to be studied under these conditions. When the observed rate constants (k_{obs}) were plotted against the ferrocenes concentration, excellent linear dependencies were observed, and the second-order rate constants for the one-electron oxidation of the ferrocene donors by the *N*-oxyl radicals (k_{et}) were obtained from the slopes of these plots. The plots of k_{obs} *vs.* [FcX] for the reactions of SINO (**1**) are shown in Fig. 3.

Table 3 Oxidation potentials of ferrocenes (FcX) in CH_3CN (E°), and second-order rate constants (k_{ET}) for the reaction of FcX with *N*-oxyl radicals **1–4** in CH_3CN at 25 °C[a]

		k_{et} ($M^{-1}s^{-1}$)[d]			
		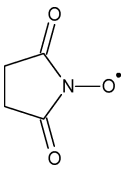	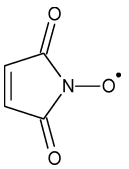	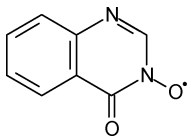	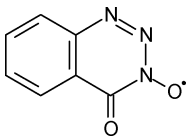
FcX	E° (V *vs.* SCE)[b]	SINO (0.92 V)[e]	MINO (0.77 V)[e]	QONO (0.84 V)[e]	BONO (0.77 V)[e]
FcH	0.41	$9.9 \pm 0.2 \times 10^7$	$4.9 \pm 0.3 \times 10^5$	$7.8 \pm 0.4 \times 10^8$	$> 2 \times 10^9$
$FcMe_2$	0.29	$3.8 \pm 0.2 \times 10^8$	$8.1 \pm 0.9 \times 10^6$	$1.8 \pm 0.1 \times 10^9$	n.d.
FcEt	0.34	$1.9 \pm 0.1 \times 10^8$	$2.0 \pm 0.1 \times 10^6$	$9.2 \pm 0.3 \times 10^8$	n.d.
$FcCH_2OH$	0.40	$1.3 \pm 0.1 \times 10^8$	$2.1 \pm 0.2 \times 10^6$	$7.7 \pm 0.5 \times 10^8$	n.d.
$FcCONH_2$	0.58	$1.2 \pm 0.1 \times 10^7$	n.d.	$3.3 \pm 0.3 \times 10^7$	$3.6 \pm 0.2 \times 10^8$
$FcCO_2Et$	0.65	$8.8 \pm 0.2 \times 10^5$	n.d.	n.d.	$1.05 \pm 0.08 \times 10^8$
FcCOMe	0.66	n.d.	n.d.	n.d.	$9.6 \pm 0.5 \times 10^7$
FcCOPh	0.69[c]	n.d.	n.d.	n.d.	$9.3 \pm 0.6 \times 10^7$

[a] Dicumyl peroxide (0.8 M), *N*-hydroxy derivative **1H–4H** (3.0–8.2 mM), ferrocenes (0.05–6.5 mM). [b] Ref. 11,12 [c] Ref. 22. [d] Determined by LFP from the slopes of the k_{obs} for the buildup of the ferrocenium ions (reactions with SINO, MINO and QONO radicals) or the decay of the BONO radical *vs.* the FcX concentration. [e] Reduction Potentials for *N*-oxyl Radicals *vs.* SCE, see Table 1.

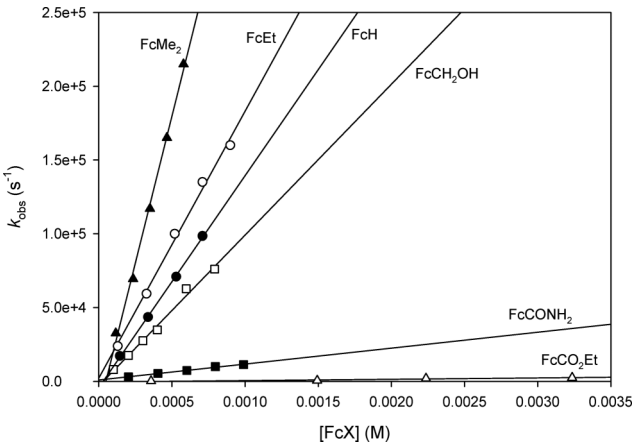

Fig. 3 Plots of the observed rate constant (k_{obs}) against [FcX] for the reactions of the SINO radical measured in argon-saturated MeCN solution at $T = 25$ °C, following the buildup of the ferrocenium ions. The slope of the plots gives the k_{ET} values.

Additional plots for the reactions investigated are reported in the ESI (Figures S8–S10‡).

All the kinetic data are collected in Table 3, where the redox potentials of the ferrocene donors are also included.

Discussion

The data in Table 3 show that the second-order rate constants for the electron transfer from substituted ferrocenes to the *N*-oxyl radicals **1–4** (k_{et}) are very sensitive to the oxidation potential of the substrate increasing by decreasing the E° value of FcX, *i.e.* as the free energy change of the ET step (ΔG°_{et}) decreases (ΔG°_{et} values are reported in Table S1 in the ESI‡). If we compare the reactivity of the different aminoxyl radicals with the unsubstituted FcH we can observe that the highest k_{et} value is observed with the BONO radical ($> 2 \times 10^9$ $M^{-1}s^{-1}$) which is characterized by the lowest redox potential in the series of *N*-oxyl radicals **1–4**. Moreover the BONO radical is much more reactive than the MINO radical even though they have similar redox potentials. The SINO radical is less reactive than the BONO and the QONO radicals even though it is characterized by the highest redox potential of the series (0.92 V *vs.* SCE). The same conclusions can be drawn if we compare the ET reactivity of **1–4** with the substituted ferrocenes.

Interestingly, similar results were observed in the ET process from substituted ferrocenes to the PINO and BTNO radicals.[12] As already mentioned, PINO was found to be much less reactive than BTNO even though it is characterized by a higher redox potential. Thus, the differences in intrinsic ET reactivity of **1–4** can be put on a quantitative basis by determining the intrinsic barrier for the $R_2NO^\bullet/R_2NO^-$ couples. To this purpose the ln k_{et} values were plotted against $\Delta G^{\circ\prime}$ that is the free energy change of the ET step corrected for the electrostatic contribution arising from the charge variation in the reactants upon electron transfer (details of calculation and $\Delta G^{\circ\prime}$ values are reported in Table S1 in the ESI‡) according to eqn (5), which combines the Marcus and Eyring equations.[23,24] In eqn (5) λ is the reorganization energy and Z is the bimolecular collision frequency. Satisfactory fits of the experimental data to eqn (5) have been observed for all the radicals, as shown in Fig. 4 for the SINO radical ($r^2 = 0.944$) and in Figures S11–S13 in the ESI for the MINO, QONO and BONO radicals.‡

$$k_{et} = Ze^{-\frac{(\lambda+\Delta G^{\circ\prime})^2}{4\lambda RT}} \quad (5)$$

From the nonlinear least-squares fitting, the λ values reported in Table 4 have been calculated for the reorganization energy required in the ET from ferrocene derivatives to *N*-oxyl radicals **1–4**.

Assuming that the value of the ET self-exchange reorganization energy for the ferrocene/ferrocenium couple ($\lambda_{Fc^+/Fc}$) is 27.5 kcal mol^{-1} in MeCN,[11] the reorganization energies for the $R_2NO^\bullet/R_2NO^-$ couples ($\lambda_{NO^\bullet/NO^-}$) can be calculated from eqn (6).

Table 4 Reorganization energies (λ) for the reaction of *N*-oxyl radicals **1–4** with substituted ferrocenes in CH_3CN at 25 °C and self-exchange ET reorganization energies of the $R_2NO^{\bullet}/R_2NO^-$ couples ($\lambda_{NO^{\bullet}/NO^-}$)

Substrate	λ^a	$\lambda_{NO^{\bullet}/NO^-}{}^a$
SINO (**1**)	43.6	59.7
MINO (**2**)	49.4	71.3
QONO (**3**)	36.0	44.5
BONO (**4**)	27.9	28.3
PINO	38.3[b]	49.1[b]
BTNO	31.1[c]	34.7[c]

[a] In kcal mol^{-1}. [b] Ref. 11 [c] Ref. 12.

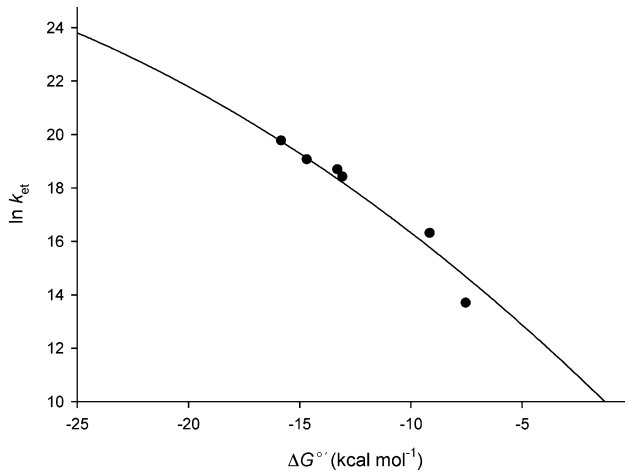

Fig. 4 Diagram of lnk_{et} *vs.* $\Delta G^{\circ\prime}$ for the reactions of substituted ferrocenes with SINO. The solid circles correspond to the experimental values; the curve is calculated by nonlinear least-squares fit to eqn (5).

The $\lambda_{NO^{\bullet}/NO^-}$ values are reported in Table 4 together with those previously determined for the PINO and BTNO radicals.[11,12] The $\lambda_{PINO/PINO^-}$ and $\lambda_{BTNO/BTNO^-}$ are within the range of $\lambda_{NO^{\bullet}/NO^-}$ values determined in this study.

$$\lambda = 1/2\ (\lambda_{NO^{\bullet}/NO^-} + \lambda_{Fc^+/Fc}) \quad (6)$$

Considering the entire series of *N*-oxyl radicals in Table 4, we note that the $\lambda_{NO^{\bullet}/NO^-}$ values increase in the order BONO < BTNO < QONO < PINO < SINO < MINO which clearly do not parallel the order of the oxidation potentials BTNO < PINO < BONO ≅ MINO < QONO < SINO. Thus, the kinetic barriers are sufficient to overcome the thermodynamic factor so that an *N*-oxyl radical can be a more effective ET oxidant than another *N*-oxyl radical with a higher redox potential.

Another important observation from the data reported in Table 4 concerns the profound effect of the structure on the $\lambda_{NO^{\bullet}/NO^-}$ values. It can be noted that the difference between the highest (MINO) and the lowest (BONO) $\lambda_{NO^{\bullet}/NO^-}$ value is more than 40 kcal mol^{-1}.

Even small modification of the structure of the *N*-oxyl radicals lead to significant variations of the $\lambda_{NO^{\bullet}/NO^-}$ values as found for example in the comparison of the MINO and SINO radicals. An increase of more than 10 kcal mol^{-1} in the $\lambda_{NO^{\bullet}/NO^-}$ value resulted by the insertion of a double bond in the five membered ring. An even more substantial increase of the $\lambda_{NO^{\bullet}/NO^-}$ value (> 15 kcal mol^{-1}) can be observed by replacing the nitrogen atom in the benzotriazole ring of NHBO with a carbon atom in the quinazolinone system of NHQO.

A simple explanation for such remarkable structural effects on the self-exchange ET reorganization energies of the $R_2NO^{\bullet}/R_2NO^-$ couples is at present very difficult. In a previous work,[12] in order to explain the higher intrinsic reactivity of BTNO with respect to PINO in ET reactions from ferrocenes, we proposed that the higher spin delocalization in BTNO than in PINO and the higher charge delocalization in $BTNO^-$ than in $PINO^-$ might be responsible for the lower $\lambda_{NO^{\bullet}/NO^-}$ value found for the former *N*-oxyl radical. We also pointed out that spin and charge delocalization also exert their effect by influencing (decreasing) the energy associated to the solvent reorganization, which might be a very important factor in the determination of the intrinsic barrier. Tentatively, it seems that the same considerations can now be extended to the series of aminoxyl radicals investigated in this study. Thus, the higher $\lambda_{NO^{\bullet}/NO^-}$ values found for the MINO and SINO radicals might be in accordance with a probably significantly lower degree of spin delocalization in the radicals MINO and SINO[25] and charge delocalization in the anions $MINO^-$ and $SINO^-$ due to the absence of an aromatic ring in their structure. On the same line, the very small $\lambda_{NO^{\bullet}/NO^-}$ value for BONO might be attributed, at least in part, to a larger delocalization of negative charge in $BONO^-$ suggested by the relatively low pK_a value (4.0) of NHBO[26] which is even smaller than that of HBT.

Experimental section

Starting materials

CH_3CN (spectrophotometric grade) was used for all the experiments. Commercial samples of dicumyl peroxide, *N*-hydroxysuccinimide, *N*-hydroxymaleimide and 3-hydroxybenzotriazin-4-one were used as received. 3-Hydroxy-quinazolin-4-one was synthesized according to the literature.[27] Ferrocene (FcH), benzoylferrocene (FcCOPh), acetylferrocene (FcCOMe), ferrocenemethanol ($FcCH_2OH$), ethylferrocene (FcEt), 1,1′-dimethylferrocene ($FcMe_2$) are commercially available and were further purified by sublimation or by column chromatography on silica gel using toluene as eluent (FcEt). Ethyl ferrocenecarboxylate ($FcCO_2Et$) was prepared by esterification of commercially available ferrocenecarboxylic acid with ethanol according to the literature.[28]

Cyclic voltammetry

Cyclic voltammetry at the steady disk electrode (glassy carbon disk, 1.5 mm in diameter) was carried out at 25 °C in CH_3CN containing the *N*-hydroxy derivatives **1H–4H** (2.0 mM) and Bu_4NBF_4 (0.1 M) as supporting electrolyte in the presence of collidine (4 mM). A three-electrode circuit was used with a home-made potentiostat with positive feedback ohmicdrop compensation and PLI hardware (Vernier Software & Technology) controlled by a program written in C++ language for Windows 95/98. The auxiliary electrode was a platinum wire (surface 1 cm^2), and an Ag/AgCl (KCl 3 M) electrode was used as reference; the redox potential values are then referred to SCE. The sweep scan was 500 mV s^{-1}.

Laser flash photolysis experiments

Laser flash photolysis experiments were carried out with an Applied Photophysics LK-60 laser kinetic spectrometer providing 8 ns pulses, using the third armonic (355 nm) of a Quantel Brilliant-B Q-switched Nd:YAG laser. The laser energy was adjusted to ≤ 10 mJ/pulse by the use of the appropriate filter. A 3 mL Suprasil quartz cell (10 mm × 10 mm) was used for all the experiments. N_2-saturated CH_3CN solutions of dicumyl peroxide (0.8 M), *N*-hydroxy derivatives **1H–4H** (3.0–8.2 mM) and ferrocenes (0.05–6.5 mM) were used. All the experiments were carried out at T = 25 ± 0.5 °C under magnetic stirring. Data were collected at individual wavelengths with an Agilent Infinium oscilloscope and analyzed with the kinetic package implemented in the instrument. Rate constants were obtained by monitoring the change of absorbance at the maximum absorption wavelength and by averaging 3–5 values. Each kinetic trace obeyed a first-order kinetic and second order rate constants were obtained from the slopes of the plots of the observed rate constants k_{obs} *vs.* substrate concentration.

Acknowledgements

Financial support from the Ministero dell'Università e della Ricerca (MUR) is gratefully acknowledged. We thank Prof. Lorenzo Stella for the use and assistance in the use of a LFP equipment and Dr Patrizia Gentili for the technical assistance in the cyclic voltammetry.

References

1 Y. Ishii, K. Nakayama, M. Takeno, S. Sakaguchi, T. Iwahama and Y. Nishiyama, *J. Org. Chem.*, 1995, **60**, 3934; Y. Ishii, T. Iwahama, S. Sakaguchi, K. Nakayama and Y. Nishiyama, *J. Org. Chem.*, 1996, **61**, 4520; Y. Yoshino, Y. Hayashi, T. Iwahama, S. Sakaguchi and Y. Ishii, *J. Org. Chem.*, 1997, **62**, 6810; Y. Ishii, S. Sakaguchi and T. Iwahama, *Adv. Synth. Catal.*, 2001, **343**, 393; F. Minisci, F. Recupero, G. F. Pedulli and M. Lucarini, *J. Mol. Catal. A: Chem.*, 2003, **204–205**, 63–90; F. Minisci, F. Recupero, A. Cecchetto, C. Gambarotti, C. Punta and R. Paganelli, *Org. Process Res. Dev.*, 2004, **8**, 163; R. A. Sheldon and I. W. C. E. Arends, *Adv. Synth. Catal.*, 2004, **346**, 1051; G. Yang, Y. Ma and J. Xu, *J. Am. Chem. Soc.*, 2004, **126**, 10542; G. Yang, Q. Zhang, H. Miao, X. Tong and J. Xu, *Org. Lett.*, 2005, **7**, 263; F. Rajabi, J. H. Clark, B. Karimi and D. J. Macquarrie, *Org. Biomol. Chem.*, 2005, **3**, 725; Y. Aoki, S. Sakaguchi and Y. Ishii, *Tetrahedron*, 2006, **62**, 2497; Y. Ishii and S. Sakaguchi, *Catal. Today*, 2006, **117**, 105; R. A. Sheldon and I. W. C. E. Arends, *J. Mol. Catal. A: Chem.*, 2006, **251**, 200; F. Recupero and C. Punta, *Chem. Rev.*, 2007, **107**, 3800; J. M. Lee, E. J. Park, S. H. Cho and S. Chang, *J. Am. Chem. Soc.*, 2008, **130**, 7824; S. Coseri, *J. Phys. Org. Chem.*, 2009, **22**, 397; S. Coseri, *Catal. Rev.*, 2009, **51**, 218; X. Yang, L. Zhou, Y. Chen, C. Chen, Y. Su, H. Miao and J. Xu, *Catal. Commun.*, 2009, **11**, 171; X. Yang, Y. Wang, L. Zhou, C. Chen and J. Xu, *J. Chem. Technol. Biotechnol.*, 2010, **85**, 564.

2 D. S. Argyropoulos, S. B. Menachem, *Biotechnology in the Pulp and Paper Industry*, K. E. L. Eriksson, Ed., Springer-Verlag: Berlin Heidelberg, 1997, pp 127–158.

3 H. P. Call and I. Mucke, *J. Biotechnol.*, 1997, **53**, 163; K. Li, F. Xu and K.-E. L. Eriksson, *Appl. Environ. Microbiol.*, 1999, **65**, 2654; B. J. Sealey, A. J. Ragauskas and T. J. Elder, *Holzforschung*, 1999, **53**, 498; E. Srebotnik and K. E. Hammel, *J. Biotechnol.*, 2000, **81**, 179; A. Potthast, T. Rosenau and K. Fischer, *Holzforschung*, 2001, **55**, 47; M. Fabbrini, C. Galli and P. Gentili, *J. Mol. Catal. B: Enzym.*, 2002, **16**, 231; X. Geng, K. Li and F. Xu, *Appl. Microbiol. Biotechnol.*, 2004, **64**, 493; C. Annunziatini, P. Baiocco, M. F. Gerini, O. Lanzalunga and B. Sjögren, *J. Mol. Catal. B: Enzym.*, 2005, **32**, 89; F. Xu, H.-J. W. Deuss, B. Lopez, L. Lam and K. Li, *Eur. J. Biochem.*, 2001, **268**, 4169; F. D'Acunzo, P. Baiocco, M. Fabbrini, C. Galli and P. Gentili, *New J. Chem.*, 2002, **26**, 1791; G. Cantarella, C. Galli and P. Gentili, *New J. Chem.*, 2004, **28**, 366; B. Branchi, C. Galli and P. Gentili, *Org. Biomol. Chem.*, 2005, **3**, 2604; C. Bohlin, K. Lundquist and L. J. Joensson, *Bioorg. Chem.*, 2009, **37**, 143; E. M. Cadena, T. Vidal and A. L. Torres, *Bioresour. Technol.*, 2010, **101**, 8199; C. Valls, J. F. Colom, C. Baffert, I. Gimbert, M. B. Roncero and J.-C. Sigoillot, *Biochem. Eng. J.*, 2010, **49**, 401.

4 S. Witayakran and A. J. Ragauskas, *Adv. Synth. Catal.*, 2009, **351**, 1187.

5 R. Khlifi, L. Belbahri, S. Woodward, M. Ellouz, A. Dhouib, S. Sayadi and T. Mechichi, *J. Hazard. Mater.*, 2010, **175**, 802; C. Torres-Duarte, R. Roman, R. Tinoco and R. Vazquez-Duhalt, *Chemosphere*, 2009, **77**, 687.

6 (*a*) B. B. Wentzel, M. P. J. Donners, P. L. Alsters, M. C. Feiters and R. J. M. Nolte, *Tetrahedron*, 2000, **56**, 7797; (*b*) F. Minisci, C. Punta, F. Recupero, F. Fontana and G. F. Pedulli, *J. Org. Chem.*, 2002, **67**, 2671; (*c*) N. Koshino, Y. Cai and J. H. Espenson, *J. Phys. Chem. A*, 2003, **107**, 4262; (*d*) N. Koshino, B. Saha and J. H. Espenson, *J. Org. Chem.*, 2003, **68**, 9364; (*e*) F. Minisci, F. Recupero, A. Cecchetto, C. Gambarotti, C. Punta, R. Faletti, R. Paganelli and G. F. Pedulli, *Eur. J. Org. Chem.*, 2004, 109; (*f*) C. Annunziatini, M. F. Gerini, O. Lanzalunga and M. Lucarini, *J. Org. Chem.*, 2004, **69**, 3431; (*g*) Y. Cai, N. Koshino, B. Saha and J. H. Espenson, *J. Org. Chem.*, 2005, **70**, 238; (*h*) P. Brandi, C. Galli and P. Gentili, *J. Org. Chem.*, 2005, **70**, 9521; (*i*) C. Galli, P. Gentili and O. Lanzalunga, *Angew. Chem., Int. Ed.*, 2008, **47**, 4790; (*j*) A. Coniglio, C. Galli, P. Gentili and R. Vadalà, *Org. Biomol. Chem.*, 2009, **7**, 155.

7 R. Amorati, M. Lucarini, V. Mugnaini, G. F. Pedulli, F. Minisci, F. Recupero, F. Fontana, P. Astolfi and L. Greci, *J. Org. Chem.*, 2003, **68**, 1747.

8 E. Baciocchi, M. F. Gerini and O. Lanzalunga, *J. Org. Chem.*, 2004, **69**, 8863.

9 E. Baciocchi, M. Bietti, M. F. Gerini and O. Lanzalunga, *J. Org. Chem.*, 2005, **70**, 5144.

10 E. Baciocchi, M. Bietti, O. Lanzalunga, A. Lapi and D. Raponi, *J. Org. Chem.*, 2010, **75**, 1378.

11 E. Baciocchi, M. Bietti, M. Di Fusco and O. Lanzalunga, *J. Org. Chem.*, 2007, **72**, 8748.

12 E. Baciocchi, M. Bietti, M. Di Fusco, O. Lanzalunga and D. Raponi, *J. Org. Chem.*, 2009, **74**, 5576.

13 D. V. Avila, C. E. Brown, K. U. Ingold and J. Lusztyk, *J. Am. Chem. Soc.*, 1993, **115**, 466.

14 D. V. Avila, J. Lusztyk and K. U. Ingold, *J. Am. Chem. Soc.*, 1992, **114**, 6576; D. V. Avila, K. U. Ingold, A. A. Di Nardo, F. Zerbetto, M. Z. Zgierki and J. Lusztyk, *J. Am. Chem. Soc.*, 1995, **117**, 2711.

15 Experimental measurements of the NO–H BDE of **1H–4H** by the EPR equilibration technique was not possible because of the low stability of the aminoxyl radicals **1–4**.

16 G. Da Silva and J. W. Bozzelli, *J. Phys. Chem. C*, 2003, **111**, 5760.

17 R. Arnaud, A. Milet, C. Adamo, C. Einhorn and J. Einhorn, *J. Chem. Soc., Perkin Trans. 2*, 2002, 1967.

18 The calculated rate constant for the HAT from propane by SINO is ca 30 times higher than the rate of the HAT process by PINO,[19] moreover the SINO radical was also predicted to be more reactive than PINO and MINO in the HAT reaction from ethylbenzene.[17]

19 I. Hermans, P. Jacobs and J. Peeters, *Phys. Chem. Chem. Phys.*, 2007, **9**, 686.

20 The decay of the *N*-oxyl radical is not always well defined due to the weak absorption in the visible region of the spectrum.

21 J. E. Frey, L. E. Du Pont and J. J. Puckett, *J. Org. Chem.*, 1994, **59**, 5386.

22 M.-L. Abasq, M. Saidi, J. L. Burgot and A. Darchen, *J. Organomet. Chem.*, 2009, **694**, 36.

23 R. A. Marcus, *Annu. Rev. Phys. Chem.*, 1964, **15**, 155.

24 L. Eberson, *Electron Transfer Reactions in Organic Chemistry*, *Springler Verlag:* Berlin Heidelberg, 1987; Chapter 3.

25 Unfortunately, because of the relative instability of the *N*-oxyl radicals **1–4**, no experimental data are available in this respect.

26 P. Astolfi, P. Brandi, C. Galli, P. Gentili, M. F. Gerini, L. Greci and O. Lanzalunga, *New J. Chem.*, 2005, **29**, 1308.

27 A. El-Faham and F. Albericio, *Eur. J. Org. Chem.*, 2009, 1499.

28 S. Top, S. Masi and G. Jaouen, *Eur. J. Inorg. Chem.*, 2002, 1848.

